# Role of tropical lower stratospheric cooling in deep convective activity: (I) Recent trends in tropical circulation

**Kunihiko Kodera[1], Nawo Eguchi[2], Rei Ueyama[3, 4], Yuhji Kuroda[1], Chiaki Kobayashi[1], Beatriz M. Funatsu[5], and Chantal Claud[6]**

[1] Meteorological Research Institute, Tsukuba, 305-0052, Japan
[2] Research Institute for Applied Mechanics, Kyushu University, Kasuga, 816-8580, Japan
[3] NASA Ames Research Center, Moffett Field, 94035-0001, USA
[4] Bay Area Environmental Research Institute, Moffett Field, 94035-0001, USA
[5] CNRS, Université de Nantes, UMR 6554 LETG, Campus du Tertre, Nantes, 44312, France
[6] Laboratoire de Météorologie Dynamique, Ecole Polytechnique, Palaiseau, 91128, France

*Correspondence to*: Kunihiko Kodera (kodera.kk@gmail.com)

**Abstract.** Large changes in tropical circulation, in particular those related to the summer monsoon and cooling of the sea surface in the equatorial eastern Pacific, were noted from the mid to late 1990s. The cause of such recent decadal variations in the tropics was studied by making use of a meteorological reanalysis dataset. Cooling of the equatorial southeastern Pacific Ocean occurred in association with enhanced cross-equatorial southerlies, which resulted from a strengthening and poleward shift of the rising branch of the boreal summer Hadley circulation connected to the stratospheric circulation. From boreal summer to winter, the anomalous convective activity centre moves southward following the seasonal march to the equatorial Indian Ocean–Maritime Continent region, which strengthens the surface easterlies over the equatorial central Pacific. Accordingly, ocean surface cooling extends over the equatorial central Pacific. We suggest that the fundamental factor causing the recent decadal change in the tropical troposphere and the ocean is a poleward shift of the rising branch of the summertime Hadley cell, which can result from a strengthening of extreme deep convection penetrating into the tropical tropopause layer, in particular over the continents of Africa and Asia, and adjacent oceans. We conjecture that this effect is produced by a combination of land surface warming due to increased $CO_2$ and a reduction of static stability in the tropical tropopause layer due to tropical stratospheric cooling. Stratospheric variation has generally been treated as a separated problem from a recent surface climate change, but this framework may be used as working hypothesis for further study.

## 1 Introduction

Large changes in tropical circulation occurred from the mid to late 1990s. These include a slowdown, or hiatus, of global warming in association with a decrease in the tropical eastern Pacific sea surface temperature (SST) (Kosaka and Xie, 2013; England et al., 2014; Trenberth et al., 2014; Watanabe et al., 2014). Changes were also found in the advancement of the onset of the Asian summer monsoon (Kajikawa et al., 2012; Gautam and Regmi, 2013; Xiang and Wang, 2013; Yun et al., 2014) and an increase in precipitation in West Africa over the Sahel (Fontaine et al., 2011; Brandt et al., 2014; Maidment et

al., 2015, Diawara et al., 2016). An increase in precipitation in southern Africa was also noted during the austral summer (Vizy and Cook, 2016). Besides these large-scale circulation changes, changes occurred in mesoscale phenomena such as an increase in Mesoscale Convective Systems (MCSs) over Sahel (Taylor et al., 2017). The tropical cyclone frequency and intensity over the Arabian Sea (Evan and Camargo, 2011) were also reported. Wang et al. (2012) pointed out that these phenomena are, in fact, related to the abovementioned early onset of the Asian summer monsoon. A relationship between tropopause layer cooling and tropical cyclone activity in the Atlantic has also been suggested (Emanuel et al., 2013). Indeed, recent numerical model studies show that cooling of the tropopause impacts the intensity of tropical storms as well as SSTs (Ramsay, 2013; Wang et al., 2014). In this respect, the recent cooling of the tropical tropopause and lower stratosphere from around 2000 (Randel et al., 2006; Randel and Jensen, 2013) should be investigated together with tropical tropospheric change.

The importance of the Pacific Decadal Oscillation (PDO) on decadal changes in global temperature and precipitation has been noted (Meehl et al., 2013; Dong and Dai, 2015; Trenberth, 2015). The most recent hiatus ended around 2013 followed by a large warming due to an El Niño event in 2015 (Hu and Fedorov, 2017; Liu and Zhou, 2017; Urabe et al., 2017; Xie and Kosaka, 2017). However, the El Niño of 2015/16 was different from the previous large 1997/98 El Niño with less warming in the eastern Pacific (Paek et al., 2017), conforming to an increasing trend of the central Pacific-type El Niño (Kao and Yu, 2009; Johnson, 2013). In this sense, the anomalous tropical circulation from the 1990s did not terminate with the hiatus, but is persisting. Similarly, the northward shift of the convective zone in the boreal summer still continues, as shown below.

As a cause of recent tropical changes, multidecadal variations of the atmosphere–ocean coupled mode such as the Atlantic Multidecadal Oscillation have also been proposed (Wang et al., 2013; Kamae et al., 2017). The possible impact of SSTs in different oceanic basins on recent trends in monsoon precipitation was studied by using a coupled ocean model by Kamae et al. (2017). Their results show that the change in Atlantic SST can reproduce recent increasing trends in monsoon rainfall in the northern hemisphere (NH), except for the Asian monsoon. The Atlantic SSTs, however, have practically no effect on the southern hemisphere (SH) such as the African and Australian monsoons. Another difference from observations is that the simulated increase in rainfall occurs mainly over the oceans in low latitudes between the equator and 15° N rather than over continents between around 10° N and 20° N as observed (see Fig. 3 of Kamae et al., 2017). Thus, it is difficult to attribute the recent global trends to a regional mode of decadal oceanic variation alone. In this paper, we first show that the fundamental factor causing the recent decadal trend in the tropics from the mid to late 1990s is not the PDO, but rather a poleward shift of the summertime rising branch of the Hadley circulation connected to the upwelling branch of the stratosphere.

One aspect of the recent trends in tropical circulation that has been reported is the poleward expansion of the tropics (e.g., Davis and Rosenlof, 2012). The expansion of the tropics is rather related to a change in the sinking branch of the Hadley cell driven by midlatitude transient eddies (Kang and Polvani, 2011). There are also other phenomena showing large trends in high latitudes and polar regions that are a part of global change and could be related to tropical change. However, in the interest of brevity, this paper focuses on changes in the tropics.

Global climate change involves diverse aspects from the stratosphere to the ocean, from the polar region to the tropics, and from monsoon to severe storms. Each of these elements should be investigated independently in great detail, but their relationships to each other and their roles in global climate change also warrant investigation. Without the latter, we are unable to see the "big picture". Stratospheric variation has generally been treated as a separated problem from a recent surface climate change. The goal of this study is to provide a framework for putting some of the pieces together by elucidating the connection between the atmosphere and ocean in the tropics.

The paper is organized as follows. After describing the data used for the study in Sect. 2, the results of our analysis are presented in Sect. 3. Finally, a summary and discussion of the causes of the recent tropical changes are presented in Sect. 4.

## 2 Data

We make use of meteorological reanalysis data produced by the Japan Meteorological Agency (JMA), JRA55 (Kobayashi et al., 2015). A large discontinuity was found at the end of the 1990s in the previous reanalysis product, JRA25, when the TIROS Operational Vertical Sounder (TOVS) on board the National Oceanic and Atmospheric Administration (NOAA) satellite was switched to Advanced TOVS (ATOVS) (Li et al., 2000). This discontinuity has largely been reduced in the JRA55 reanalysis (Kobayashi et al., 2015). To investigate deficiencies in the general circulation model, we make use of a family of JRA55 product: AMIP-type Simulation (JRA55-AMIP), which uses the same model and boundary conditions as JRA55 reanalysis, but without assimilation of observational data in the atmosphere.

Outgoing longwave radiation (OLR) data provided by NOAA are widely used for analysis of convective activity in the tropics. In the present study, we use monthly mean OLR data (1° × 1° latitude–longitude resolution) derived from the High Resolution Infrared Radiation Sounder (HIRS) (Lee et al., 2007), available at ftp://eclipse.ncdc.noaa.gov/cdr/hirs-olr/monthly/. Analysis of the precipitation is performed by making use of Global Precipitation Climatology Project (GPCP) monthly mean data Ver.2.3 (Adler et al., 2003). COBE monthly mean gridded SST data with 1° × 1° boxes compiled by the JMA (Ishii et al., 2005) are used for the study of oceanic surface change.

Climatology is defined by the 30-year mean from 1981 to 2010 in the present study. Seven El Niño events after 1979 are defined by the JMA based on 6-monthly mean SSTs in the Niño 3 sector (5° S–5° N, 150° W–90° W) (available at http://ds.data.jma.go.jp/gmd/tcc/tcc/products/elnino/ensoevents.html). In this study, we define the NH cold seasons 1982/83, 1986/87, 1991/92, 1997/98, 2002/03, 2009/10, and 2015/16 as El Niño winters.

Detection of the tropical overshooting cloud (COV) was made according to the diagnostics developed by Hong et al. (2005), which is based on the brightness temperature differences measured by three high frequency channels of the Advanced Microwave Sensing Unit (AMSU) module B or the Microwave Humidity Sensor (MHS). The data are from NOAA and MetOp satellites: period 2007-2013 for MetOp-A and 2014-2017 for MetOp-B. Their equatorial crossing time is nearly the same (see Fig. 1 of Funatsu et al., 2016). The original data calculated with 0.25°x 0.25° grid was resampled to a coarse one of 2.5°× 2.5° for plotting purposes. Number density of COV is defined as total number of COV detected in each 2.5° x 2.5° bins divided by MetOp-MHS total pixel numbers to remove sampling bias. Units are parts per thousand.

## 3 Results

### 3.1 Surface variation vs. OLR

The recent poleward shift of the convergence zone in the boreal summer is identified from the July–September mean anomalous OLR in 1999–2016 from 30-year climatology (1981–2010) (Fig. 1a). A northward shift of the convective activity is seen around the summer monsoon regions over Africa, Asia, and Central America. A poleward shift is further evident in the zonal-mean OLR in Fig. 1b. Climatological OLR peaks around 10° N, while anomalous OLR of the recent period has a maximum around 15° N.

There is a close relationship between the position of the tropical convergence zone and the development of cold tongues in the tropical oceans. Convective activity shifts northward during boreal summer. Accordingly, cross-equatorial winds west of the American and African continents increases which lead to a decrease in the SSTs along the coastal regions during the boreal summer as a part of seasonal cycle. Thus, the primary factor producing cold tongues in the tropical SSTs is the shape of continents, air–sea interaction, and the position of the rising branch of the Hadley circulation, as described in Xie and Philander (1994) and Xie (2004). Therefore, changes in the rising branch of the Hadley circulation, such as can be seen in Fig. 1, can directly impact the equatorial eastern Pacific SSTs.

To investigate whether the northward shift of the convective zone is driven by the PDO, anomalous OLR during the two periods of neutral and negative phases of the PDO is displayed in Figs. 1c and 1d together with anomalous SSTs during those time periods (Figs. 1e and 1f). A characteristic horseshoe pattern in the north Pacific SST is evident during the

negative phase of the PDO. Anomalous OLR indicates that the convective activity is enhanced along 15 °N–20 °N latitude irrespective of the phase of the PDO, except for the sector under the direct influence of the PDO in the eastern Pacific, where cooling is larger during the negative phase. However, even during the neutral phase of the PDO, negative anomalies in the SST exist in the tropics west of South America. This suggests that the SST cooling west of South America is not solely driven by the PDO, but is related to the strengthening and northward shift of the convective activity.

The seasonal dependence of the recent trend in tropical convective activity is depicted in Fig. 2. The panels on the left show latitude–time sections of 3-monthly mean anomalous zonal-mean OLR from 1979 to 2016. To better illustrate the evolution in latitudinal structure, the tropical mean (10 °S–25 °N) is further subtracted from the temporal anomaly in Fig. 2. Inspection reveals a change in zonal-mean OLR around 1999 (vertical lines) in all four seasons: The anomalous negative zone shifts northward after 1999 from boreal spring to summer and descends to lower latitudes from boreal summer to autumn following the seasonal march.

The horizontal structure of the anomalous OLR in the recent period (1999–2016) is depicted in the panels on the right for each season: April, May and June (AMJ), July, August and September (JAS), October November and December (OND), and January, February, and March (JFM). The anomalous negative centre of OLR is located around the Maritime Continent during boreal spring, which shifts northward by spreading longitudinally along 15 °N, in particular along the African and Asian sectors during boreal summer. Next, the negative OLR region shifts and clusters over the Indian Ocean region during boreal autumn. At the same time, positive OLR anomalies develop over the equatorial eastern Pacific, suggesting a suppression of convective activity over the Pacific Ocean. During boreal winter, the anomalous convective active region shifts eastward over the Maritime Continent, and suppression of convective activity over the eastern Pacific is sustained during the cold season.

The impact of the recent decadal variation of convective activity on the SST is depicted in Fig. 3. The top panels show the 1999–2016 mean anomalous OLR in (a) JAS, (b) OND. The anomalous horizontal winds at 925 hPa and SSTs are presented in the bottom panels. Because the response of the SST arises following atmospheric circulation, anomalous SSTs during the following month (i.e., August, September and October (ASO) and November, December and January (NDJ) are displayed in Figs. 3c and 3d, respectively. In JAS, the anomalous cross-equatorial flow west of South America intensifies due to a poleward shift of a rising branch of the Hadley cell. The cross-equatorial flow changes from westward to eastward when it crosses the equator according to the change in sign of the Coriolis force. This results in a strengthening of the climatological easterlies in the SH and enhances anomalous convergence near New Guinea. In contrast, easterlies are weakened in the NH, which explains a warming in the north, but a cooling south of the equator. Such a meridional seesaw of the anomalous SSTs and cross-equatorial flow suggests an important role for wind−evaporation−SST (WES) feedback (Xie and Philander, 1994) in recent trends. The centre of anomalous negative OLR moves to the equatorial eastern Indian Ocean from boreal summer

to autumn, which results in a strengthening of anomalous easterlies over the equatorial central Pacific and a westward extension of low SSTs over the equator.

In the analysis above, two different features in decadal variability are seen, one over continental and the other over oceanic sectors. Here we examine the characteristics of the variations over the African continent (10° W–40° E) sector and the Pacific Ocean (170° W–120° W) sector, corresponding to the longitudes of Niño 3.4. To identify the different characteristics of convective activity over continents and ocean, the climatological annual cycle in the zonal mean pressure vertical velocity at 300 hPa is depicted in Figs. 4a and 5a. A region of enhanced convective activity migrates north and south over the continent following the seasonal variation of solar heating. It should be noted that the convective zone over Africa shows a jump during the summer monsoon season (Hagos and Cook, 2007). In the case of the Pacific Ocean, the convective zone shows only a small latitudinal excursion and is located in the NH around 5° N throughout the year.

Latitude–time sections of the 3-monthly mean anomalous (departures from climatology) 300 hPa pressure vertical velocity are shown from February 1979 to November 2016 over the African sector in Fig. 4b. The vertical velocity increases from the mid-1990s in both hemispheres around 10°−20° in latitude corresponding to the rising branch of the summertime Hadley circulation in the TTL. Accordingly, the annual mean precipitation over Africa increases in the recent period (1999−2016) in both hemispheres over the Sahel and Namibia.

Over the Pacific Ocean sector (Fig. 5b), strong upward motion appears over the equator when El Niño events occur. The anomalous region of upward motion, however, tends to stay north of the equator after 1999. Accordingly, the annual mean anomalous precipitation during the recent period exhibits a large increase around 5° N−10° N, but decreases over the equator and the SH (Fig. 5c). This change in the atmospheric response to the El Niño event is related to the change in the strength of the cross-equatorial winds (Fig. 5d). After 1999, although SSTs increased over the equator during El Niño, the anomalous northward wind remained stronger and the convective activity tended to stayed in the NH.

Latitude−time section of 3-monthly anomalous SST of the Niño 3.4 sector (Fig. 5f) show little change in latitudinal structure. Figure 5e shows a longitude–time section of the anomalous OLR over the equatorial SH (0°–10° S). The impact of cooling of the eastern equatorial Pacific in the SH can also be seen as a structural change in El Niño/Southern Oscillation (ENSO) phenomena after 1999. Convective activity largely increases over the Pacific during El Niño events before 1999. However, after 1999, Pacific convective activity is suppressed; an increase in convective activity during El Niño is apparent only over the central Pacific. In contrast, convective activity west of 160° E over the Maritime Continent generally increases after 1999. Such changes should be connected with a decadal change in anomalous zonal winds over the tropical SH (10° S−5° N) (Fig. 5f), which can be related to an increased cross-equatorial southerlies through the effect of the Coriolis force.

### 3.2 S-T coupling

In addition to the change in the troposphere, increasing trend in the tropical lower stratospheric upwelling at 70 hPa, together with the increasing number of sudden stratospheric warming events, was identified by Abalos et al. (2015). A height–time section of the zonal mean temperature around the tropopause, together with the zonally averaged pressure vertical velocity at 70 hPa, shows year-to-year variation of the temperature associated with the quasi-biennial oscillation superimposed on a decadal cooling trend in the lower stratosphere. In the upper troposphere, warming pulses related to El Niño events are superimposed on a warming trend in the troposphere (Fig. 6). A decrease in lower stratospheric temperature and an increase of upper tropospheric temperature lead to a decrease in the static stability of the TTL. It has been suggested that increased stratospheric tropical upwelling tends to enhance deep convective activity, in particular deep penetrating clouds, through change in the static stability of the TTL (Eguchi et al., 2015; Kodera et al., 2015). In the following we will examine how the decadal variation in the stratosphere and troposphere is connected.

For this, singular value decomposition (SVD) analysis (Kuroda, 1998) was conducted based on the normalized covariance matrix between the zonal mean pressure vertical velocity and the horizontal distribution of the OLR or SST in the tropics (30° S–30° N) during boreal summer (JAS) (Fig. 7). Each value at the grid point was weighted by the layer thickness in vertical, and the cosine of the latitude in meridional direction. To investigate the relative importance of zonal mean vertical velocity in different altitude, the SVD calculation are made with the zonal mean pressure vertical velocity of (a) 150–50 hPa and (b) 1000–300 hPa levels. To get a general view of the entire troposphere and stratosphere, the heterogeneous correlation of the vertical velocity is extended to a height range of 1000 to 10 hPa. The levels used for the SVD calculation are indicated by arrows. A variation related to the decadal variation and ENSO cycle appear as first two modes. Here we show only those related to the decadal variation. Increasing trends in coefficients are evident in two cases. However, zonal mean ω around 15° N-20° N is much closely related to the variation around the TTL (Fig. 7a) than variation in the lower troposphere (Fig. 7b). Accordingly, the variation of the OLR around 15° N over African-Asian sector is more closely related with the vertical velocity around the TTL. In the case of the SVD with tropospheric vertical velocity, heterogeneous correlation with OLR show the relationship with convective activity over equatorial Pacific north of the equator which is mainly confined within the troposphere. Therefore these results suggest a stronger connection between convective activity around the rising branch of the Hadley circulation and the lower stratospheric circulation as suggested in previous works (Eguchi et al, 2015; and Kodera et al., 2015).

### 3.3 Variation over continent and ocean

Tropospheric zonal mean vertical velocity shows relatively small connection with the horizontal distribution of the OLR. This can be resulted from the fact that the regional scale variation dominates in the lower troposphere due to the surface geography. Therefore, meridional sections of "standardized" mean JAS 1999–2016 anomalous pressure vertical velocity

were calculated in different sectors (Fig. 8). In the case of standardized anomalies of 17-year mean as in Fig. 8, if one assumes a normal distribution, absolute values larger than 0.5 are statistically different from 0 at the 95% confidence level.

Top panel shows the zonal mean field which can be comparable to that extracted by the SVD analysis in Fig. 7a. Contours indicate climatology. Middle panels are the same as the top panel, but divided into two parts: (left) African-Asian continental sector (30° W–130°E ) and (right) Pacific-Atlantic oceanic sector (130° E–330° E). Strengthening of the upward velocity in the TTL and the lower stratosphere occurs in the continental sector adding to the northward shift in the troposphere, but over the oceanic sector, strengthening of vertical velocity occurs around 5° N-10 °N without latitudinal shift. In the oceanic sector, upwelling is largest around 5° N–10° N, and strengthening of the upwelling occurs at the same location as the climatology. If we limit the sector only over the African continent (20° W–20° E) to exclude Indian Ocean influence, the abovementioned continental characteristics becomes further clear (bottom left). Over the oceanic sector, increase of the vertical velocity occurs around 5 °N (bottom- right), but in the western Pacific sector (130° E– 170° E), upward velocity mainly develops south of the equator (10° S– 0°) (bottom- middle). We also note that in climatological vertical velocity in the western Pacific sector is confined practically in the lower troposphere over the equatorial SH (10° S– 0°). This feature can be attributed to the fact that the convergence of the air occurs over a warm ocean east of New Guinea island (Fig. 3c). This result indicates that in spite of the mixture of different profile according sectors, the zonal mean vertical field in the TTL mainly reflects the variation over African-Asian continental sector.

Continuity in a zonally averaged field does not necessarily mean actual continuity at each location as shown in the above analysis. To investigate more in detail the continuity within the rising branch of the Hadley circulation from the upper troposphere to the stratosphere, longitude−height sections of the normalized anomalous pressure vertical velocities averaged over 10°−20° latitudes in the summer hemisphere are displayed in top panels in Fig. 9 a and 9b. While bottom panels show a distribution of climatological (2007−2017) occurrence frequency of the convective over shooting (COV) in the same latitudinal zone. Inspection reveals that increasing trend of the upwelling occurs over the continental sector, especially where COVs are frequent. This characteristics are commonly seen in both summer hemispheres. The contrast between the continental and oceanic sectors is clearer in the SH where the distribution of lands is simpler. Because the COV occurs in the deep convective clouds penetrating into the TTL beyond the level of neutral buoyancy, such the increased vertical velocity in the TTL over the region of frequent COV seems reasonable. It should also be noted that a connection between the COV and the vertical velocity in the tropical lower stratosphere in day-to-day scale has been shown in a previous study by Kodera et al. (2015).

To get insight into stratosphere-related variation in the troposphere, the JAS mean vertical pressure velocity ($\omega$) at 30 hPa averaged over tropical SH (0°–25° S) is chosen as the index of stratospheric mean meridional circulation ($I_\omega$) (Fig. 10a). The correlation coefficient between $I_\omega$ and zonal mean $\omega$ at each grid point (Fig. 10b) shows a correlation pattern very similar to

the SVD mode in Fig. 7a. To indicate the relationship between the climatological residual mean-meridional circulation, the mass-weighted stream function diagnosed by the method of Iwasaki (1992) is displayed by contours in Figs. 10b and 10c. We can see that the variation in stratospheric upwelling in the Brewer–Dobson circulation is connected to the Hadley circulation in the TTL around 15° N.

The correlation between $I_\omega$ with zonal-mean temperature at each grid point from the 90° S to 90° N, is shown in Fig. 9c. The tropical upwelling is not only related to a cooling in the tropics and the summer hemisphere, but it is also related to a warming in the downwelling region around the winter polar stratosphere (Fig. 10c). This illustrates the dynamical nature of the recent tropical stratospheric cooling. Stratospheric upwelling is also connected with convective activity along 15° N−20° N (Fig. 10d), as already discussed above. The correlation coefficients between $I_\omega$ and 925 hPa zonal and meridional winds at each grid point are shown by arrows in Fig. 10e. An increase in the cross-equatorial winds in the eastern Pacific and Atlantic is observed. The impact of near surface wind variation on the SST can be seen in the lagged correlation with the SST in Fig. 10e. The cooling in the equatorial eastern Pacific is largest with a time lag of 5 months (i.e., December, January and February (DJF), consistent with the development of La Niña–like SSTs from boreal autumn in Fig. 3.

The results of above analyses can be schematically summarized in Fig. 11–left. According to this, we selected 4 key variables which can be considered as fundamental in the recent tropical trends: (a) tropical lower stratospheric temperature in early summer (temperature at 70 h Pa averaged over 20° S–20° N from 16 July-16 August), (b) pressure vertical velocity at the bottom of the TTL (150 hPa) in August, (c) August-October mean "southward" winds south of the equator (10° S–0°) in the western hemisphere (180° W–0°) , (d) tendency in the SST, from the early summer (May-July) to late autumn (October–December) in the tropical Pacific west of South American continent (15° S–5° S, 100° W–80° W). Time series of these 4 variables (a–d) are displayed in Fig 11–right. When all 4 variables become negative (indicated by red dots), we define this as negative event. Similarly when all variables become positive (black dot), it is defined as positive event. All 6 positive events occurred within the first 14 years, while all 7 negative events appeared during the last 13 years. Chi-square test was conducted to examine whether such distribution of the events occurs by chance by dividing the whole 39 years to 3 equal period of 13-year. The result ($\chi^2 = 23$) indicates that such distribution occurs by chance with less than 0.1% of probability. Therefore, there is a statistically significant tendency that negative events occur more frequently in recent decade.

The problem here is, however, whether there is a causal relationship among the variables. We introduced a seasonal variation for the selection of the variable from the stratospheric cooling at the end of July, to a cooling of ocean from summer to autumn. This time evolution tentatively suggests a causality among them, however, more exact study is needed to really demonstrate.

**4. Summary and discussion**

Characteristics of the recent tropical circulation change from the middle to the end of the 1990s can be summarized as follows. Decadal cooling in the eastern Pacific occurs in relationship with an increase in cross-equatorial winds, and the easterlies in the tropical SH, which is also related with a strengthening of the convective activity over the African-Asian sector during the boreal summer (Fig. 3). Also, a correlation analysis (Fig. 10) indicates that these variation in the convective activity and the SSTs are related with the vertical velocity around the tropopause levels.

Although it is difficult to demonstrate the causal relationship statistically among the variables exhibiting large trends, such as (a) lower stratospheric temperature, (b) upwelling in the TTL, (c) cross-equatorial winds near surface, and (d) SST tendency from boreal summer to autumn in Fig. 11, they could be related by following processes: The relationship between the convective activity in the rising branch of the Hadley circulation and the cooling of the tropical eastern Pacific can be explained according to the work of Xie (2004) involving a wind−evaporation−SST (WES) feedback. Connection between the tropical stratospheric cooling and the extreme deep convection around rising branch of the Hadley cell in summer hemisphere has been suggested in previous studies (Eguchi et al., 2015; Kodera et al., 2015). Therefore, a combination of these two processes can be used as a "working hypothesis" for the recent tropical change as in Fig. 11.

Although the period of observation may be too short, Aumann and Ruzmaikin (2013) reported that the tropical deep convection over land shows an increasing trend, while that over oceans shows an decreasing trend based on 10 years of Atmospheric Infrared Sounder (AIRS). Furthermore, Taylor et al. (2017) showed that intense mesoscale convective system of which cloud top temperature lower than -70° C largely increased over the Sahel since 1982. The temperature of −70° C corresponds approximately to the air temperature at 150 hPa. This means that the extreme deep convection penetrating to the TTL largely increased over African continent consistent with the present study.

For the study of the causal relationship, numerical model simulation is usually performed. For this, however, model should be able to reproduce correctly involved key processes, which should be extreme deep convection penetrating to the TTL in the present case. To examine the model performance, we compare the climatological mean vertical velocities around the TTL from the JRA55 reanalysis and the JRA55-AMIP run. The latter uses the same atmospheric general circulation model and boundary conditions (SST and sea ice) as JRA55, but without the assimilation of observed data (Kobayashi and Iwasaki, 2016). Usually, the difference arises from the model deficiency. In JRA55-AMIP, upwelling in the summer tropics and downwelling in the winter polar stratosphere are weaker (Fig. 12a). The horizontal distribution of the difference in pressure vertical velocity at 150 hPa (lower panels in Fig. 12a) show that model upwelling is weaker in summer over land and adjacent oceans around 10°–20° in latitude. Regions of weak upwelling in the model coincide with the regions of increasing

recent decadal trends in upwelling. Because the observed change is rather opposite to the model biases, it is possible that current models may not properly simulate the recent trends in the tropics.

Concerning to the origin of trend, the increasing trend in the Earth's surface temperature is generally attributed to the increase in greenhouse gases like $CO_2$ (IPCC, 2013). Such a change in the radiative forcing may explain the global characteristics of the recent change. The effect of increased $CO_2$ can be divided into a direct radiative effect and an indirect effect through changes in the SST. Model experiments have shown that the direct radiative effect of $CO_2$ increases tropical upward motion particularly over the Sahelian sector, whereas it suppresses upwelling over the oceanic sector in the Pacific (Fig. 8 of Gaetani et al., 2016). An increase in $CO_2$ raises the Earth's surface temperature, but also decreases stratospheric temperatures. Note, however, that the recent cooling in the lower stratosphere–tropopause region is also due to a dynamical effect (Abalos et al., 2015). The sudden decrease in lower stratospheric water vapour around the year 2000 (Randel et al., 2006; Hasebe and Noguchi, 2016) suggests a dynamical forcing of the change. Further investigation is needed to determine whether the stratosphere is merely passively responding to the tropospheric warming or playing an active role in the tropospheric circulation change.

Studies of long-term trends face problems that often arise from changes in the observation systems, stations or the drift of the orbit of the satellites. Therefore, to avoid these problems and to better understand the stratosphere–troposphere coupling processes, we conducted additional case studies on the northward shift of convective activity similar to that associated with the recent trend, but associated with a sudden cooling of the tropical stratosphere during a boreal summer by using convective overshooting and cloud top data derived from recent satellite observations (paper in preparation).

## 5 Data availability

Datasets used in this paper are all publicly available. Meteorological reanalysis datasets created by JMA, JRA55, and JRA-AMIP are available from http://search.diasjp.net/en/dataset/JRA55 and http://search.diasjp.net/en/dataset/JRA55_AMIP, respectively. The COBE monthly mean SST dataset can be obtained from the JMA website (http://ds.data.jma.go.jp/tcc/tcc/products/elnino/cobesst/cobe-sst.html). Monthly mean HIRS OLR data can be obtained from NOAA by FTP (ftp://eclipse.ncdc.noaa.gov/cdr/hirs-olr/monthly/). The GPCP monthly mean precipitation dataset is obtained from the NOAA website (https://www.esrl.noaa.gov/psd/data/gridded/data.gpcp). AMSU/MHS data are available at NOAA's Comprehensive Large Array Data Stewardship System. In this work, AMSU/MHS raw data were obtained with support from the INSU-CNES French Mixed Service Unit ICARE/climserv/AERIS and accessed with the help of ESPRI/IPSL.

**Acknowledgements**

The authors wish to express their thanks to Leonhard Pfister for valuable discussions and comments. This work was supported in part by Grants-in-Aid for Scientific Research (25340010, 26281016, and 16H01184) from the Japan Society for Promotion of Science.

## References

Abalos, M., Legras, B., Ploeger, F., and Randel, W.J.: Evaluating the advective Brewer-Dobson circulation in three reanalyses for the period 1979–2012, J. Geophys. Res. Atmos.,120, doi:10.1002/2015JD02, 2015.

Adler, R.F., Huffman, G.J., Chang, A., Ferraro, R., Xie, P., Janowiak, J.E., Rudolf, B., Schneider U., Curtis, S., Bolvin. D.T., Gruber, A., Susskind, J., Arkin, P.A., and Nelkin, E.J.: The Version 2 Global Precipitation Climatology Project (GPCP) monthly precipitation analysis (1979-present), J. Hydrometeor, 4, 1147-1167, 2003.

Aumann, H.H. and Ruzmaikin, A.: Frequency of deep convective clouds in the tropical zone from 10 years of AIRS data, Atmos. Chem. Phys., 13, 10795–10806, doi:10.5194/acp-13-10795-2013, 2013.

Brandt, M., Mbow, C., Diouf, A.A., Verger, A., Samimi, C., and Fensholt, R.: Ground and satellite based evidence of the biophysical mechanisms behind the greening Sahel, Global Change Biol., 21, 1–11, doi:10.1111/gcb.12807, 2014.

Davis, S.M. and Rosenlof, K.H.: A multidiagnostic intercomparison of tropical-width time series using reanalyses and satellite observations, J. Clim., 25, 1061-1078, 2012.

Diawara, A., Tachibana, Y., Oshima, K., Nishikawa, H., and Ando, Y.: Synchrony of trend shifts in Sahel boreal summer rainfall and global oceanic evaporation 1950–2012, Hydrol. Earth Syst. Sci., 20, 3789–3798, doi:10.5194/hess-20-3789-2016, 2016.

Dong, B. and Dai, A.: The influence of the interdecadal Pacific oscillation on temperature and precipitation over the globe, Climate Dyn, 45(9-10):2667–2681, 2015.

Eguchi, N., Kodera, K., and Nasuno, T.: A global non-hydrostatic model study of a downward coupling through the tropical tropopause layer during a stratospheric sudden warming, Atmos. Chem. Phys., 15, 297–304, 2015.

Emanuel, K., Solomon, S., Folini, D., Davis, S., and Cagnazzo, C.: Influence of tropical tropopause layer cooling on Atlantic hurricane activity, J. Clim., 26, 2288–2301, https://doi.org/10.1175/JCLI-D-12-00242.1, 2013.

England, M.H., McGregor, S., Spence, P., Meehl, G.A., Timmermann, A., Cai, W., Gupta, A.S., McPhaden, M.J., Purich, A., and Santoso, A.: Recent intensification of wind-driven circulation in the Pacific and the ongoing warming hiatus, Nat. Clim.Change, 4, 222–227, doi:10.1038/nclimate2106, 2014.

Evan, A.T. and Camargo, S. J. A: climatology of Arabian Sea cyclonic storms, J. Clim.24, 140–158, 2011.

Fontaine, B., Roucou, P., Gaetani, M., and Marteau, R.: Recent changes in precipitation, ITCZ convection and northern tropical circulation over North Africa (1979–2007), Int. J. Climatol., 31, 633–648, doi:10.1002/joc.2108, 2011.

Gaetani, M., Flamant, C., Bastin, S., Janicot, S., Lavaysse, C., Hourdin, F., Braconnot, P., and Bony, S.: West African monsoon dynamics and precipitation: the competition between global SST warming and CO2 increase in CMIP5 idealized simulations, Clim Dyn., doi:10.1007/s00382-016-3146-z, 2016.

Gautam, D.K. and Regmi, S.K.: Recent trends in the onset and withdrawal of summer monsoon over Nepal, ECOPERSIA, 1(4): 353-367, 2013.

Hagos, S.M. and Cook, K.H.: Dynamics of the West African monsoon jump, J Clim., 20, 5264–5284. doi:10.1175/2007JCLI1533.1, 2007.

Hasebe, F. and Noguchi, T.: A Lagrangian description on the troposphere-to-stratosphere transport changes associated with the stratospheric water drop around the year 2000, Atmos. Chem. Phys., 16, 4235-4249, doi:10.5194/acp-16-4235-2016, 2016.

Hong, G., Heygster, G., Miao, J., and Kunzi, K.: Detection of tropical deep convective clouds from AMSU-B water vapor channels measurements, J. Geophys. Res., 110, D05205, doi:10.1029/2004JD004949, 2005.

Hu, S. and Fedorov, A.V.: The extreme El Niño of 2015–2016 and the end of global warming hiatus, Geophys. Res. Lett., 44, doi:10.1002/2017GL072908, 2017.

IPCC: Summary for Policymakers. In: Climate Change 2013: The Physical Science Basis. Contribution of Working Group I to the Fifth Assessment Report of the Intergovernmental Panel on Climate Change, Stocker, T.F., Qin, D., Plattner, G.-K., Tignor, M., Allen, S.K., Boschung, J., Nauels, A., Xia, Y., Bex, V., Midgley, P.M. (eds.), Cambridge University Press, Cambridge, United Kingdom and New York, NY, USA, 2013.

Ishii, M., Shouji, A., Sugimoto, S., and Matsumoto, T.: Objective analyses of sea-surface temperature and marine meteorological variables for the 20th century using ICOADS and the KOBE collection, Int. J. Climatol., 25, 865-879, 2005.

Iwasaki, T. (1992), General circulation diagnosis in the pressure-isentrope hybrid vertical coordinate, J. Meteorol. Soc. Jpn., 70, 673–687, 1992.

Johnson, N.C.: How many ENSO flavors can we distinguish? J. Clim. ,26, 4816–4827, doi:10.1175/JCLI-D-12-00649.1., 2013.

Kajikawa, Y., Yasunari, T., Yoshida, S., and Fujinami, H.: Advanced Asian summer monsoon onset in recent decades, Geophys. Res. Lett., 39, L03803, doi:10.1029/2011GL050540, 2012.

Kamae, Y., X. Li, S.-P. Xie, and Ueda, H.: Atlantic effects on recent decadal trends in global monsoon, Clim. Dyn.., doi:10.1007/s00382-017-3522-3, 2017.

Kang, S. M., and Polvani, L.M.: The interannual relationship between the latitude of the eddy-driven jet and the edge of the Hadley cell, J. Clim., 24, 564–568, 2011.

Kao, H-Y., and Yu, J-Y.: Contrasting eastern‐Pacific and central‐Pacific types of ENSO, J. Clim., 22, 615– 632, doi:10.1175/2008JCLI2309.1., 2009.

Kobayashi, C., and T. Iwasaki: Brewer-Dobson circulation diagnosed from JRA-55, J. Geophys. Res. Atmos., 121, doi:10.1002/2015JD023476, 2016.

Kobayashi, S., Ota, Y., Harada, Y., Ebita, A., Moriya, M., Onoda, H., Onogi, K., Kamahori, H., Kobayashi, C., Endo, H., Miyaoka, K., and Takahashi, K.: The JRA-55 Reanalysis: general specifications and basic characteristics, J. Meteorol. Soc. Japan, 93, 5−48, doi:10.2151/jmsj.2015-001, 2015.

Kodera, K., Funatsu, B.M., Claud, C., and Eguchi, N.: The role of convective overshooting clouds in tropical stratosphere–troposphere dynamical coupling, Atmos. Chem. Phys., 15, 6767-6774, doi:10.5194/acp-15-6767-2015, 2015.

Kodera, K., Ueyama, R., Funatsu, B., Eguchi, N., Pfister, L., and Claud, C.,: Impact of tropical lower stratospheric cooling on deep convective activity: (II) Abrupt seasonal transition in boreal summer monsoon, in preparation, 2018.

Kosaka, Y. and Xie, S.-P.: Recent global-warming hiatus tied to equatorial Pacific surface cooling, Nature, 501, 403–407, doi:https://doi.org/10.1038/nature12534, 2013.

Kuroda, Y., An effective SVD calculation method for climate analysis, J. Meteorol. Soc. Jpn., 76, 647-655, 1998.

Lee, H., Gruber, A., Ellingson, R.G., and Laszlo, I.: Development of the HIRS outgoing longwave radiation climate dataset. J. Atmos. Oceanic Technol., 24, 2029–2047, doi: 10.1175/2007JTECHA989.1, 2007.

Li, J., Wolf, W.W., Menzel, W.P., Zhang, W., Huang, H., and Achtor, T.H.: Global soundings of the atmosphere from ATOVS measurements: The algorithm and validation, J. Appl. Meteor., 39, 1248–1268, doi.org/10.1175/1520-0450(2000)039<1248:GSOTAF>2.0.CO;2, 2000.

Liu, B. and Zhou, T., Atmospheric footprint of the recent warming slowdown, Scientific Reports, 7, 40947, doi:10.1038/srep40947, 2017.

Maidment, R.I., Allan, R.P., and Black, E.: Recent observed and simulated changes in precipitation over Africa, Geophys. Res. Lett., 42, 8155–8164, doi:10.1002/2015GL065765, 2015.

Meehl, G.A., Hu, A., Arblaster, J.M., Fasullo, J., and Trenberth, K.E.: Externally forced and internally generated decadal climate variability associated with the interdecadal Pacific oscillation, J. Clim., 26, 7298–7310, doi:10.1175/JCLI-D-12-00548.1., 2013.

Paek, H., Yu, J.-Y., and Qian, C.: Why were the 2015/2016 and 1997/1998 extreme El Niños different? Geophys. Res. Lett., 44, doi:10.1002/2016GL071515, 2017.

Ramsay, H.: The effects of imposed stratospheric cooling on the maximum intensity of tropical cyclones in axisymmetric radiative–convective equilibrium, J. Clim., 26, 9977–9985, doi: 10.1175/JCLI-D-13-00195.1., 2013.

Randel, W.J. and Jensen, E.J. : Physical processes in the tropical tropopause layer and their roles in a changing climate, Nat. Geosci., 6, 169–176, doi:10.1038/ngeo1733, 2013.

Randel, W.J., Wu, F., Vömel, H., Nedoluha, G.E., and Forster, P.: Decreases in stratospheric water vapor after 2001: links to changes in the tropical tropopause and the Brewer–Dobson circulation, J. Geophys. Res., 111, D12312, doi:10.1029/2005JD006744, 2006.

Taylor, C.M., Belušić, D., Guichard, F., Parker, D.J., Vischel, T., Bock, O., Harris, P.P., Janicot, S., Klein, C., Panthou, G.: Frequency of extreme Sahelian storms tripled since 1982 in satellite observations. Nature, 544, 475–478, https://doi.org/10.1038/nature22069, 2017.

Trenberth, K. E.: Has there been a hiatus? Science, 349(6249), 691–692, 2015.

Trenberth, K. E., Fasullo, J.T., Branstator, G. and, Phillips, A.: Seasonal aspects of the recent pause in surface warming, Nat. Clim. Change, doi:10.1038/nclimate2341, 2014.

Urabe, Y., Yasuda, T., and Maeda, S.: Rapid warming in global sea surface temperature since around 2013, SOLA, 13, 25−30, doi:10.2151/sola.2017-005., 2017.

Vizy, E.K., and Cook, K.H.: Understanding long-term (1982–2013) multi-decadal change in the equatorial and subtropical South Atlantic climate, Clim. Dyn., 46: 2087, doi:10.1007/s00382-015-2691-1, 2016.

Wang, B., Xu, S., and Wu, L.: Intensified Arabian Sea tropical storms, Nature 489, E1–E2, doi:10.1038/nature11470, 2012.

Wang, B., Liu, J., Kim, H-J,, Webster, P.J., Yim, S-Y., and Xiang, B.: Northern Hemisphere summer monsoon intensified by mega-El Niño/southern oscillation and Atlantic multidecadal oscillation, Proc Natl Acad Sci U S A, 110, 5347–5352, 2013.

Wang, S., Camargo, S.J., Sobel, A.H., and Polvani, LM.: Impact of the tropopause temperature on the intensity of tropical cyclones—an idealized study using a mesoscale mode, J. Atmos. Sci., 71, 4333–4348, 2014.

Watanabe, M., Shiogama, H., Tabete, H., Hayashi, M., Ishii, M., and Kimoto, M.: Contribution of natural decadal variability to global warming acceleration and hiatus, Nat. Clim. Change, doi:10.1038/nclimate2355, 2014.

Xiang, B. and Wang, B.: Mechanisms for the advanced Asian summer monsoon onset since the mid-to-late 1990s, J. Clim., 26, 1993–2009, 2013.

Xie, S.-P.: The shape of continents, air-sea interaction, and the rising branch of the Hadley circulation, in The Hadley Circulation, Past, Present and Future, edited by: Diaz, H. F. and Bradley, R. S., Kluwer Academic Publishers, Dordrecht, the Netherlands, 121–152, 2004.

Xie, S.-P. and Kosaka, Y.: What caused the global surface warming hiatus of 1998–2013? Curr. Clim. Change Rep., doi:10.1007/s40641-017-0063-0, 2017.

Xie, S.-P. and Philander, S.G.H.: A coupled ocean-atmosphere model of relevance to the ITCZ in the eastern Pacific, Tellus, 46A, 340−350, 1994.

Yun, K.-S., Lee, J.-Y., and Ha, K.-J.: Recent intensification of the South and East Asian monsoon contrast associated with an increase in the zonal tropical SST gradient, J. Geophys. Res. Atmos., 119, 8104–8116, doi:10.1002/2014JD021692, 2014.

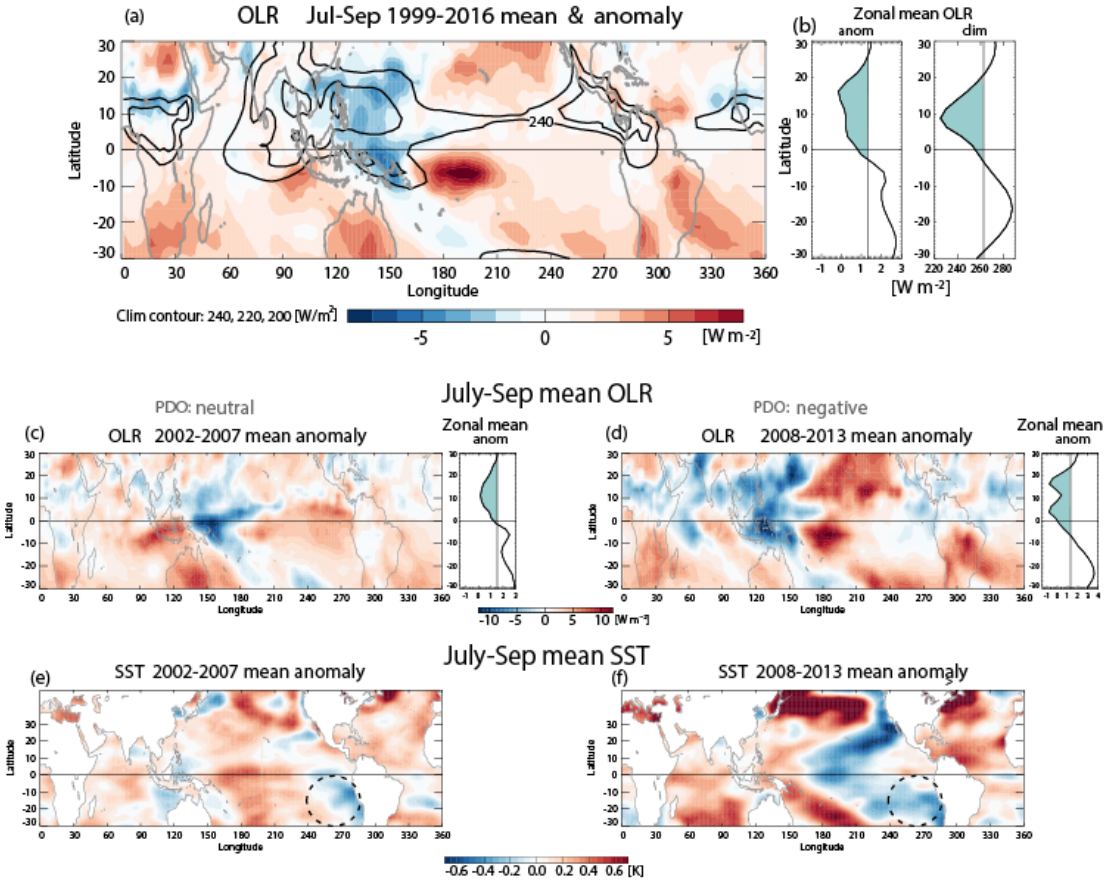


**Figure 1: (a) Climatological (1981-2010) July–September mean OLR (contours: 240, 220, and 200 W m$^{-2}$) and anomalous July–September OLR (departures from climatology) in 1999-2016 (color shading). (b) Zonal mean profiles of (a): anomalies from climatology (left) and climatology (right). (c) Anomalous OLR as in (a) and (b, left) but for 2002-2007 period. (d) Anomalous OLR as in (a) and (b, left) but for 2008-2013 period. (e,f) Anomalous July–September SST (departures from climatology) in 2002-2007 (e) and 2008-2013 (f).**

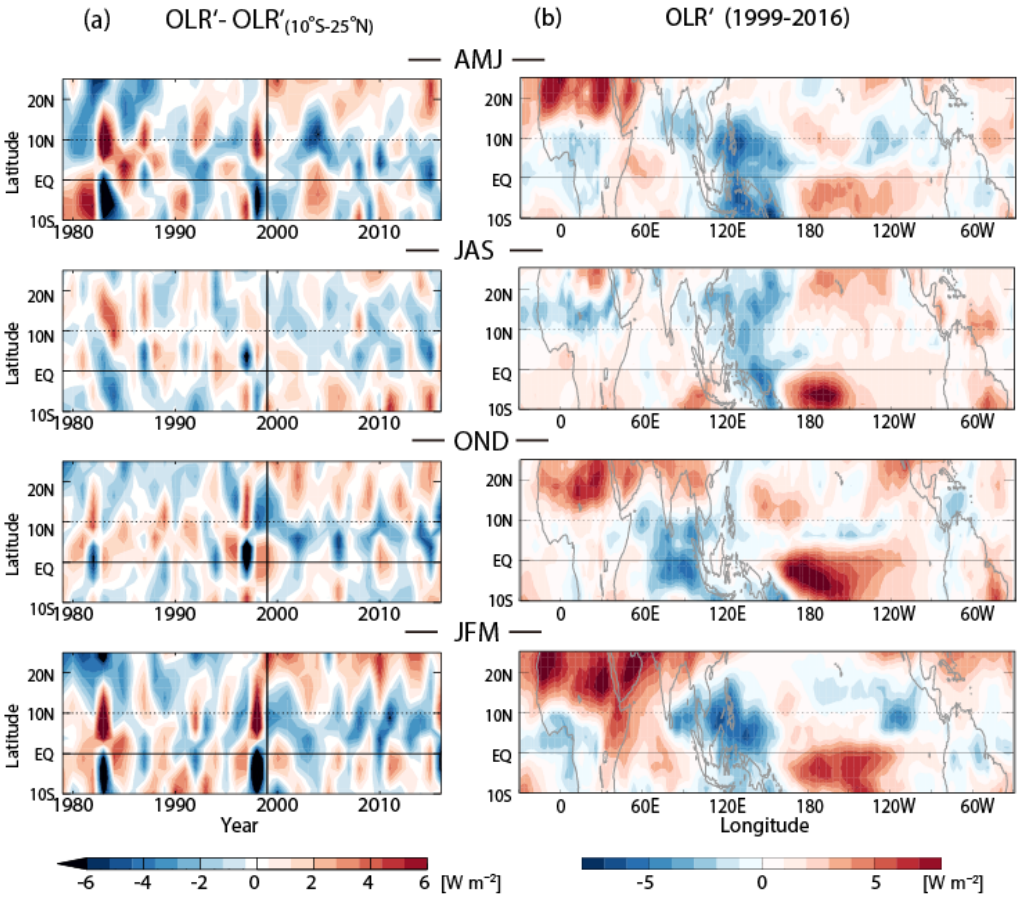


**Figure 2: (a) Latitude–time sections of 3-month seasonal mean, zonally-averaged anomalous (departures from 1981-2010 climatological tropical 10° S–25° N mean) OLR in 1979-2016. Vertical solid lines indicate the year 1999. (b) Horizontal distributions of 3-month seasonal mean anomalous OLR from climatology during 1999/2000–2015/2016 period.**

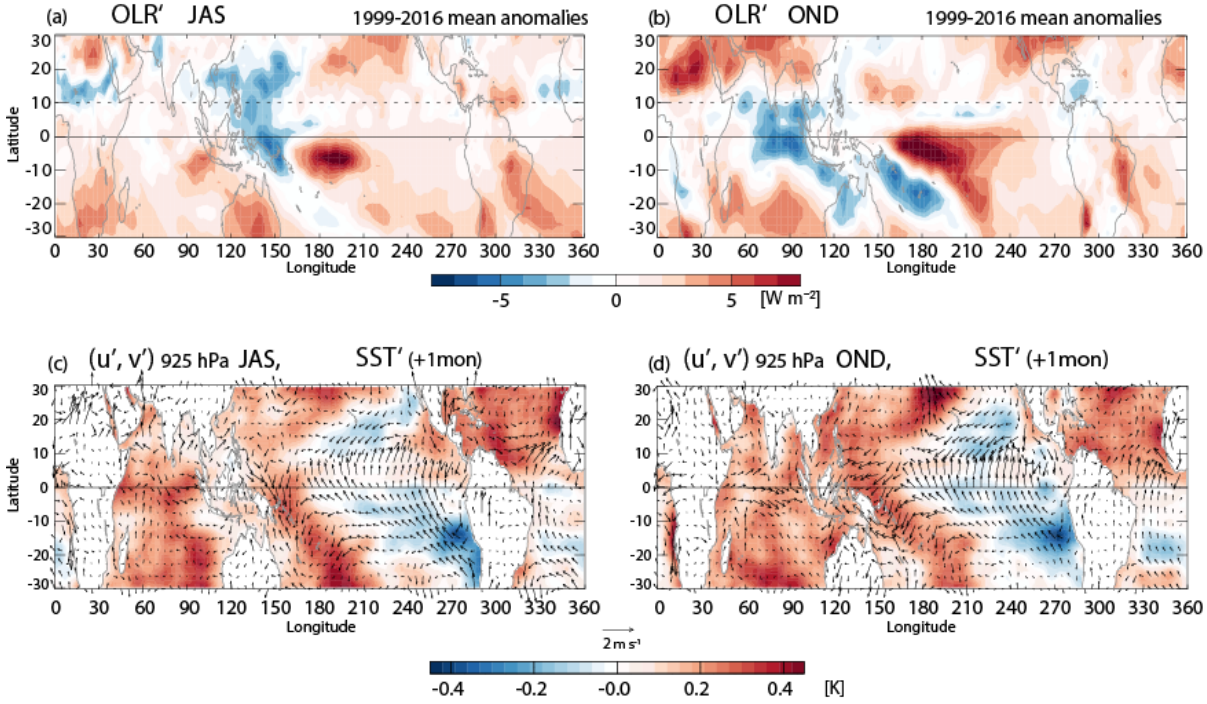


**Figure 3: (a) JAS and (b) OND mean anomalous OLR for the period 1999-2016. (c) JAS and (d) OND mean anomalous horizontal winds at 925 hPa (arrows) for the period 1999–2016 superimposed on anomalous SSTs (color shading) with a one-month lag (i.e., ASO and NDJ, respectively).**

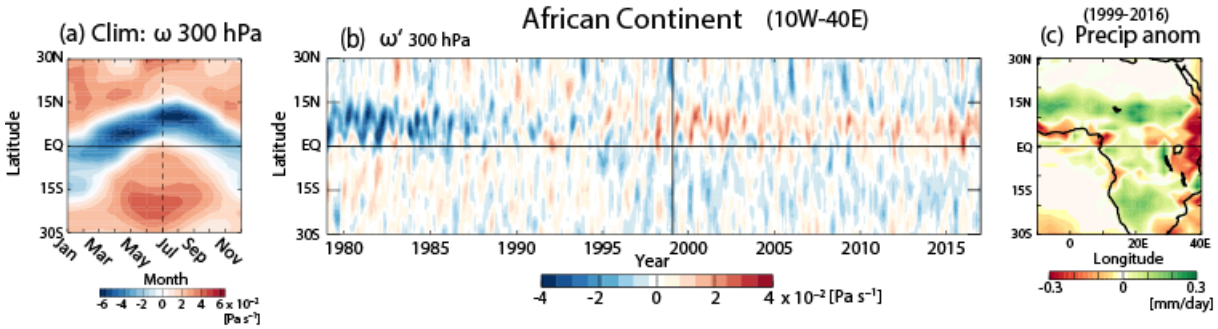


**Figure 4: (a) Latitude–time section of the climatological zonal-mean pressure vertical velocity at 300 hPa averaged over the African sector (10° W–40° E). (b) Latitude–time section of monthly mean anomalous pressure vertical velocity from February 1979 to November 2016. (c) Latitude–longitude map of annual mean anomalous precipitation during 1999–2016 over the African sector. Three monthly running mean has been applied on data prior to the presentation for (b).**

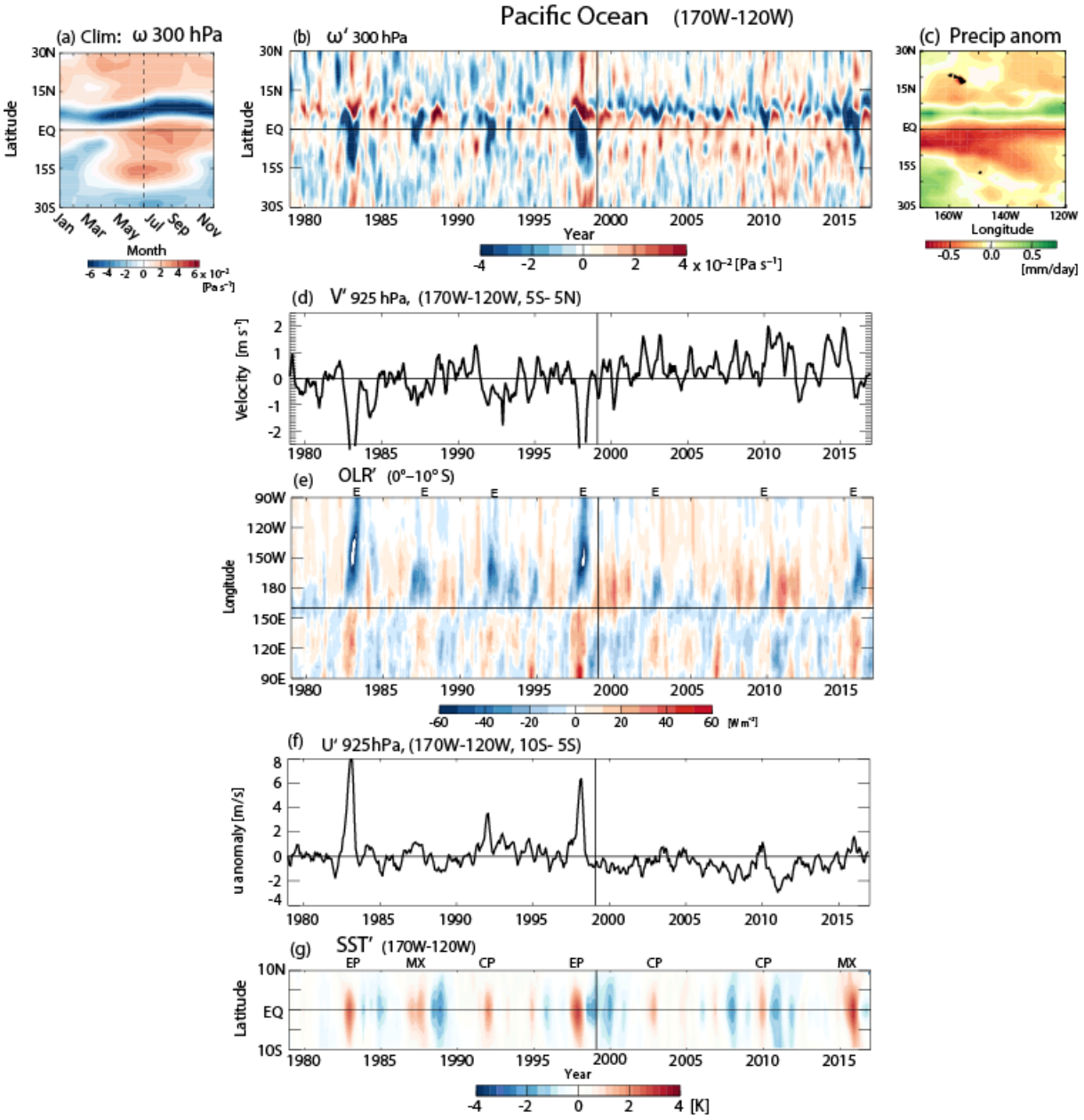


**Figure 5: (a- c) Same as in Fig. 4 except for the eastern Pacific, Niño 3.4 (170° W–120° W) sector. (d) Monthly mean anomalous meridional wind component around the Equator (5° S–5° N) over the Niño 3.4 sector. (e) Similar to (a), except for the time-longitude section of OLR around the Equator (5° S–5° N) over the Indian Ocean–Pacific sector. (f) Same as (d), except for zonal wind component around tropical SH (10° S–5° S). (g) Monthly mean anomalous SST over the Nino 3.4 sector. "EP", "CP", and "MX" indicate different types of El Niño events (Peak et al., 2017): EP, eastern Pacific; CP, central Pacific; MX, mixed type.**

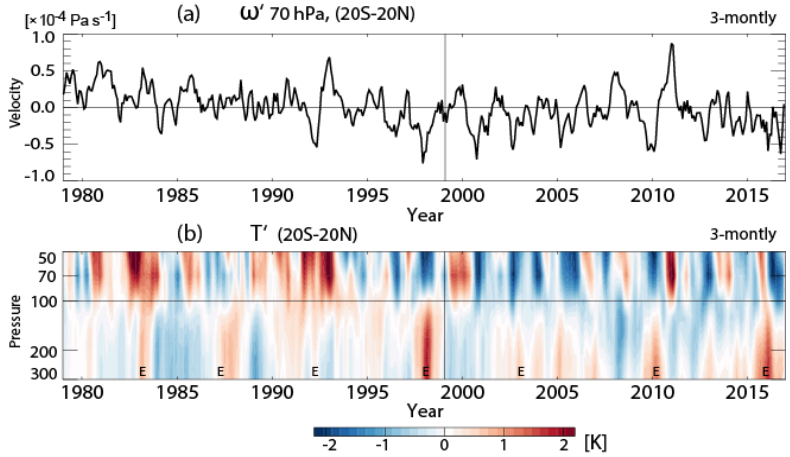


**Figure 6: (a) 3-month mean anomalous pressure vertical velocity in the tropics (20° S–20° N) at 70 hPa. (b) Height–time section of 3-month mean anomalous temperature in the tropics (20° S–20° N). "E" denotes an El Niño event.**

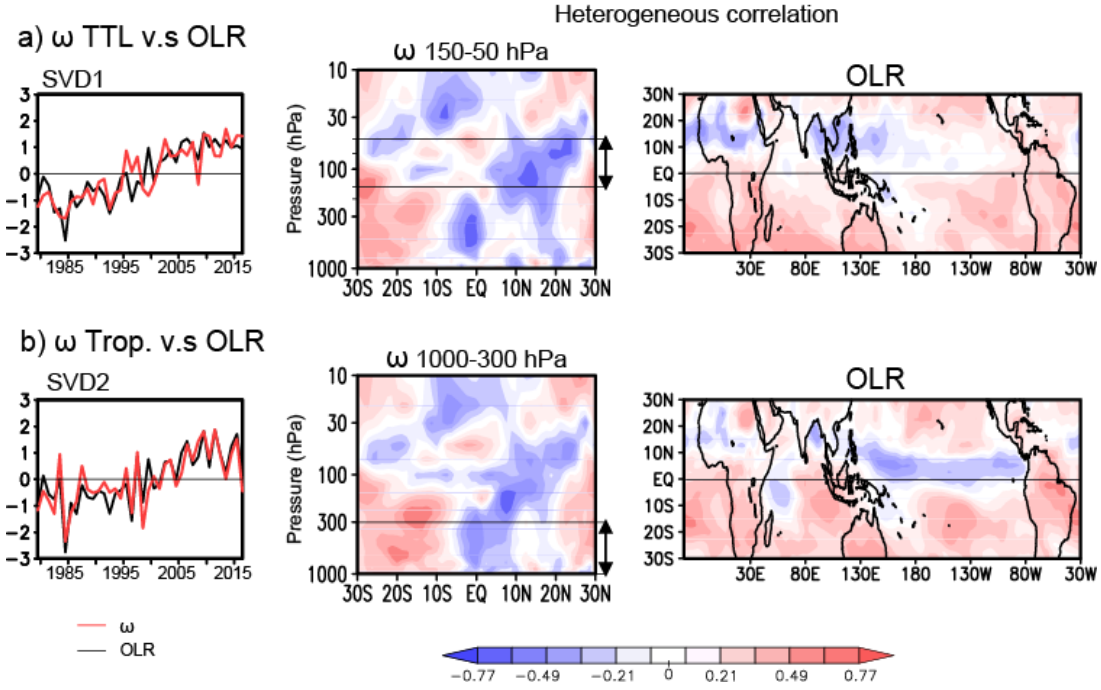


**Figure 7: SVD analysis of the zonal mean anomalous pressure velocity and anomalous OLR (0°–360° E) in the tropics (30° S–30° N) during JAS from 1979 to 2016. (a) SVD1 of pressure velocity around the TTL (50–150 hPa) (b) SVD2 of pressure velocity in the troposphere (1000–300 hPa). (from left to right) time coefficients, heterogeneous correlation of OLRs, and heterogeneous correlation map of the pressure velocity extended to 1000–10 hPa. Arrows indicate the levels used for the calculation of the SVD.**

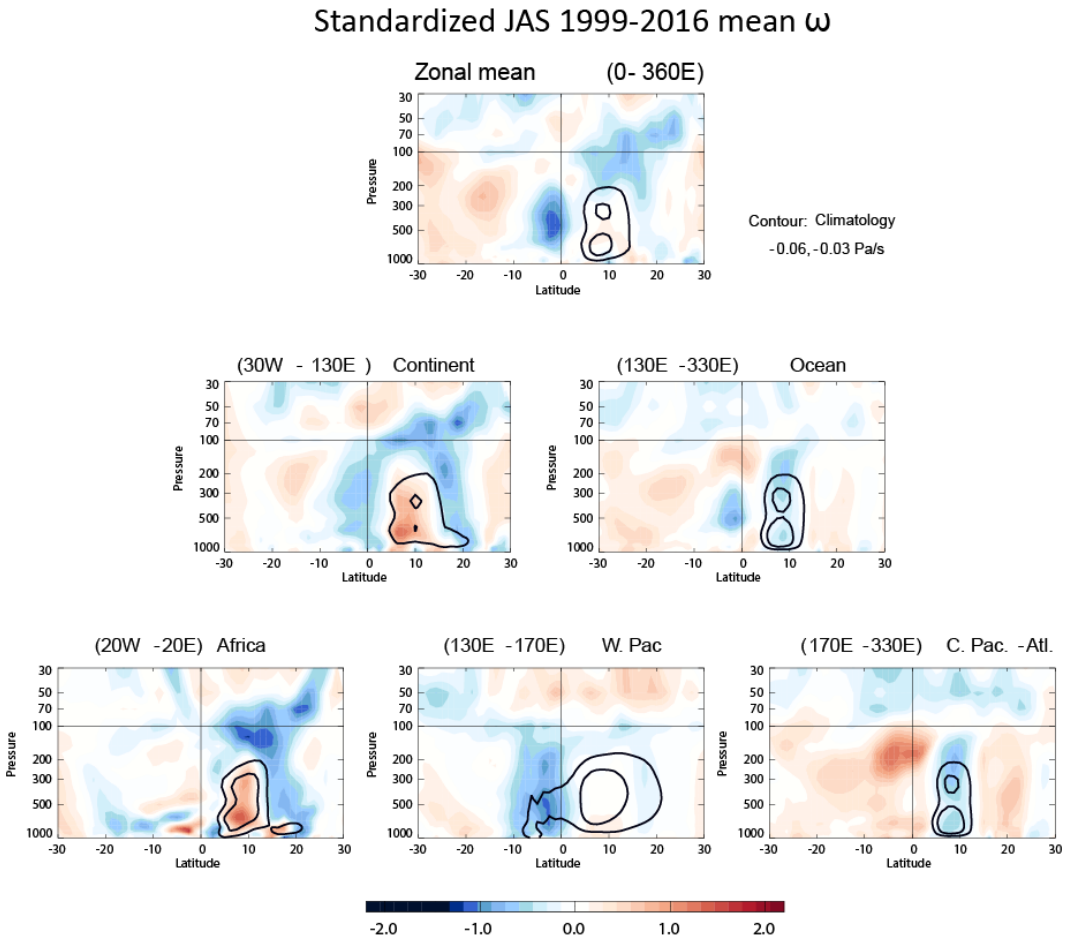


**Figure 8: (Top) Standardized anomalous OLR in JAS 1999-2016 (departures from 1981-2010 climatology). Climatological JAS mean, zonal mean pressure velocity is indicated as contours (–0.06 and–0.03 Pa $s^{-1}$). Middle panels: Same as the top panel, except for (left) African-Asian continental sector (30° W–130° E ) and (right) Pacific-Atlantic oceanic sector (130° E–330° E). Bottom panels: Same as the top panels, but for (left) African continent (20° W– 20° E ) sector, (middle) Western Pacific sector (130° E–170° E), and (right) Central Pacific–Atlantic (170° E– 330° E) sector.**

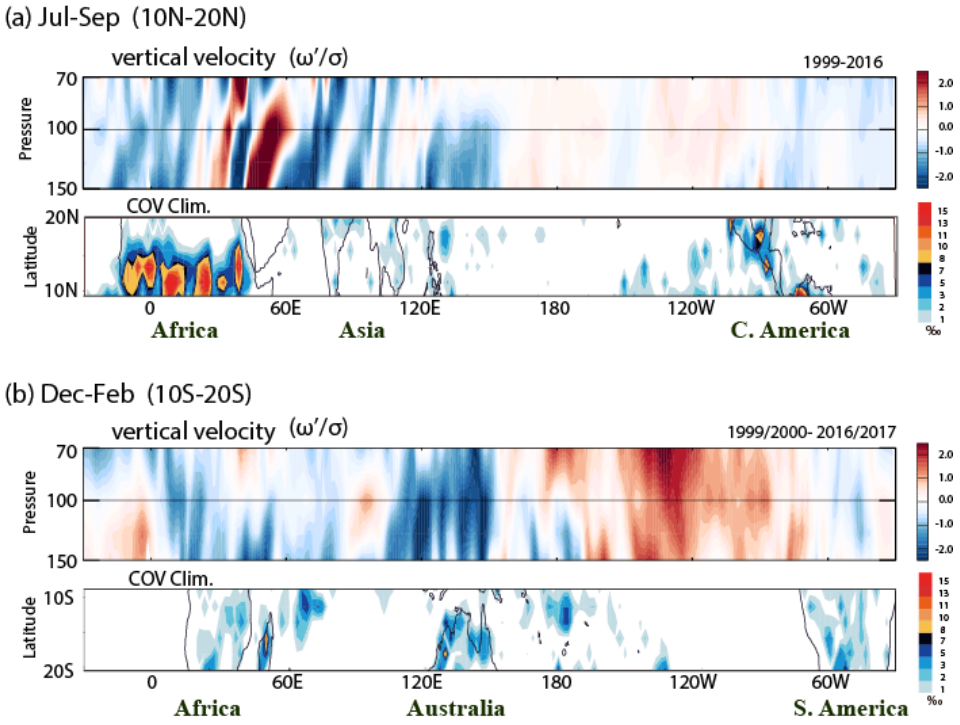


**Figure 9: (a) (top panel) Height–longitude section of the standardized (with respect to the interannual variation) anomalous pressure vertical velocity averaged over 10° N–20° N, during boreal summer (JAS) 1999–2016. (bottom panel) Climatological (2007–20017) occurrence frequency of the convective over shooting (COV) in the same latitudinal zone. Unit is parts per thousand. (b) As in (a), but for 10° S–20° S in austral summer (DJF).**

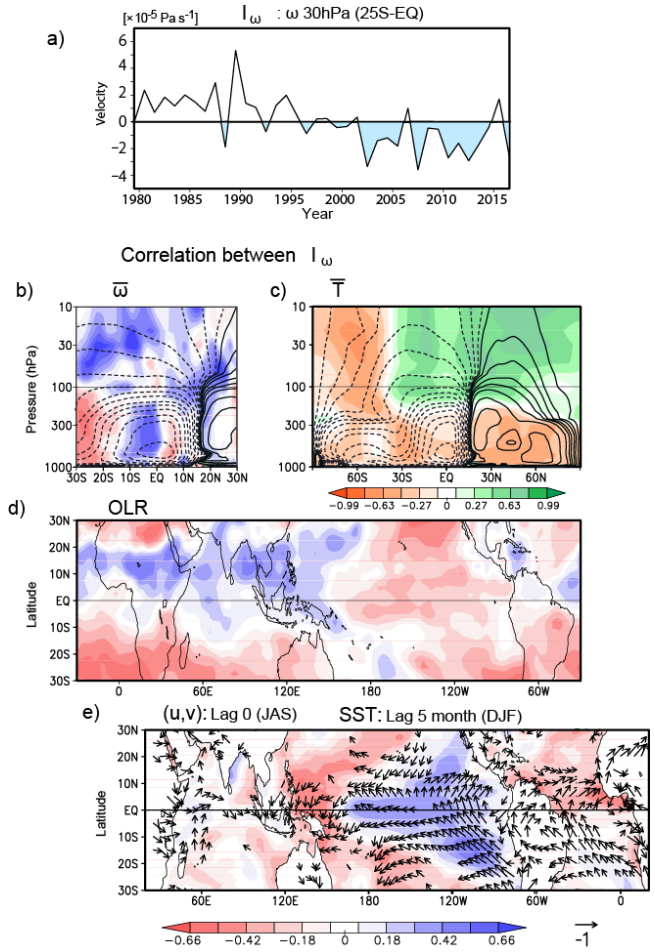


**Figure 10: (a) Time series of JAS mean vertical pressure velocity ($\omega$) at 30 hPa averaged over 0°–25° S as an index for the tropical stratospheric vertical velocity ($I_\omega$). Correlation coefficients between $I_\omega$ and (b) zonal mean $\omega$, (c) zonal mean temperature $T$ at each grid, (d) OLR, and (e) horizontal winds at 925 hPa (arrows). Lagged correlation with DJF mean SST is also presented as colored shading in (e). Contours in (b) and (c) indicate the climatological residual mean meridional circulation in JAS. Solid and dashed lines indicate clockwise and counterclockwise directions, respectively.**

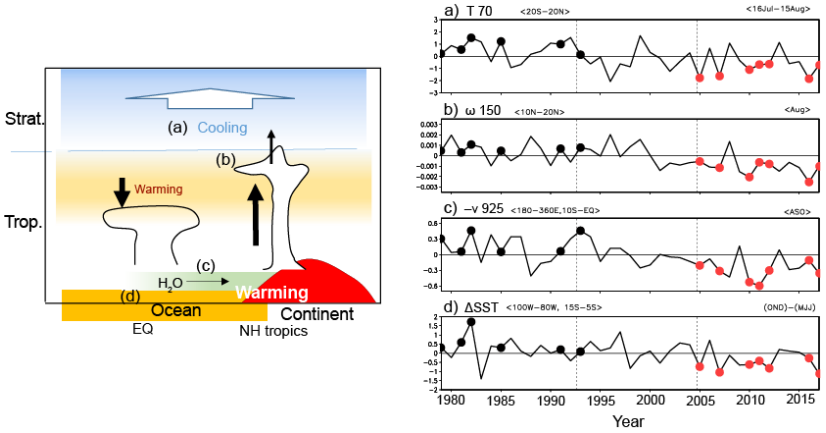


**Figure 11: (left) Schematic of the recent changes in the tropics (see text). (a-c) indicate the location of the variable shown in the right panels. (Right) Time series of 4 key variables as departure from the climatology: (a) lower stratospheric temperature, (b) upwelling in the TTL, (c) cross-equatorial winds near surface, (d) SST tendency from summer to autumn. Black and red dots indicate the cases when 4 variables are same polarity–positive or negative polarity, respectively.**

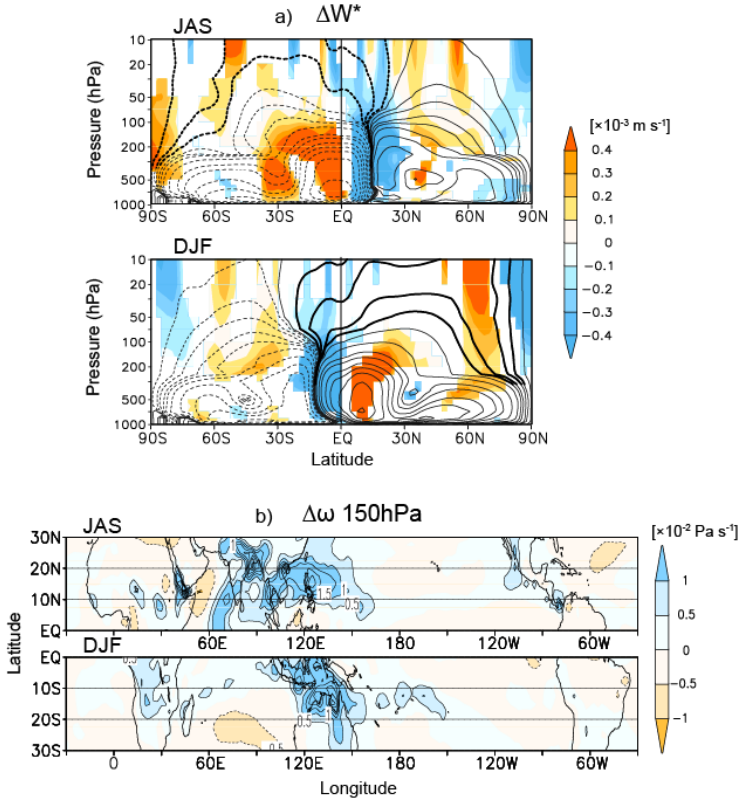


**Figure 12: (a) Difference in the climatological JAS (top) and DJF (bottom) mean residual vertical velocity between JRA55-AMIP and JRA55 reanalyses (color shading). Contours indicate the mass stream function of the mean residual circulation in JRA55-AMIP. Streamlines connected to the winter polar stratosphere from the tropics are highlighted using thick lines. Solid and dashed lines represent clockwise and counterclockwise circulations, respectively. Statistically significant differences are indicated in color. (b) Difference in pressure vertical velocity at 150 hPa between JRA55-AMIP and JRA55 reanalyses in the summer tropics: (top) JAS in the NH and (bottom) DJF in the SH.**